Journal of Atmospheric and Terrestrial Physics, Vol. 48, Nos 11–12, pp. 1145–1151, 1986.
Printed in Great Britain.

0021–9169/86 $3.00 + .00
Pergamon Journals Ltd.

Diagnostic analysis of two-dimensional monthly average ozone balance with Chapman chemistry

RICHARD S. STOLARSKI, CHARLES H. JACKMAN and JACK A. KAYE

Atmospheric Chemistry and Dynamics Branch, Code 616, NASA/Goddard Space Flight Center, Greenbelt, MD 20771, U.S.A.

(*Received for publication* 10 *March* 1986)

Abstract—Chapman chemistry has been used in a two-dimensional model to simulate ozone balance phenomenology. The similarity between regions of ozone production and loss calculated using Chapman chemistry and those computed using LIMS and SAMS data with a photochemical equilibrium model indicate that such simplified chemistry is useful in studying gross features in stratospheric ozone balance. Net ozone production or loss rates are brought about by departures from the photochemical equilibrium (PCE) condition. If transport drives ozone above its PCE condition, then photochemical loss dominates production. If transport drives ozone below its PCE condition, then photochemical production dominates loss. Gross features of ozone loss/production (L/P) inferred for the real atmosphere from data are also simulated using only eddy diffusion. This indicates that one must be careful in assigning a transport scheme for a two-dimensional model that mimics only behavior of the observed ozone L/P.

INTRODUCTION

In a previous paper (JACKMAN *et al.*, 1986) the stratospheric ozone balance was assessed from LIMS and SAMS data using a photochemical equilibrium (PCE) model for stratospheric chemistry. The results confirmed the upper stratospheric problem in which models tend to calculate less ozone than is seen by measurements (see also FREDERICK *et al.*, 1984; CRUTZEN and SCHMAILZL, 1983; other references in JACKMAN *et al.*, 1986). This was manifested by a calculated loss term in excess of production by some 40–60%. The uncertainties in the calculation were a factor of 1.7, thus the ozone imbalance was within the uncertainties. Due to the complexity of the chemistry in the upper stratosphere it was not possible to isolate the cause of this substantial imbalance.

One persistent feature of the middle stratospheric ozone balance as determined from measurements was a minimum in the ratio loss/production (L/P) of about 0.2 which was centered just above 100 mbar, with values less than 1 (indicating an excess of production over loss) extending from about 10 mbar downward to about 200 mbar. The latitudinal extent of this net production region was approximately $\pm 40°$, with a clear seasonal shift following the changing zenith angle of the sun.

Detailed interpretation of these data is difficult because of the size of the calculated upper stratospheric imbalance, which was found to occur where photochemical equilibrium is expected. The quantity of interest in the continuity equation for ozone (or, more precisely, odd oxygen, which is equal to $O_3 + O(^3P) + O(^1D)$ in an oxygen only atmosphere) is $P - L$. Because both P and L are growing rapidly with height into the upper stratosphere, $P - L$ may also grow rapidly if there is any imbalance in its calculation from data, due to inaccuracies in the data themselves or any of the photochemical parameters involved in its calculation. In order to alleviate this problem and attempt to interpret the calculated production and loss rates in the middle and lower stratosphere, a two-dimensional model was used which included only minimal chemistry.

A key factor in understanding derived production-minus-loss curves is the realization that the sign of $P - L$ is determined by whether the ozone at a particular point at a particular time is above or below the photochemical concentration for the conditions at that point and time. To carry out an analysis of the reasons for departure from photochemical equilibrium at any time it is necessary to use a model for which a photochemical equilibrium calculation can be made which is consistent with the calculation using the full continuity equation.

We used the 2D model of GUTHRIE *et al.* (1984) with only the Chapman mechanism of pure oxygen chemistry included (shown in Table 1). This simple chemistry has the virtue of a readily defined photochemical equilibrium which does not require the

Table 1. Reactions and their rates*

Number	Reaction	Rate coefficient
(R1)	$O_2+h\nu \rightarrow O+O$	$J_1 < 242$ nm
(R2)	$O_3+h\nu \rightarrow O_2+O(^1D)$†	$J_2 < 310$ nm
(R3)	$O_3+h\nu \rightarrow O_2+O$	$J_3 < 1140$ nm
(R4)	$O+O_3 \rightarrow O_2+O_2$	$k_4 = 8.0(-12)\exp(-2060/T)$‡
(R5)	$O+O_2+M \rightarrow O_3+M$	k_5 see JPL—85-37
(R6)	$O(^1D)+O_2 \rightarrow O+O_2$	$k_6 = 3.2(-11)\exp(67/T)$
(R7)	$O(^1D)+N_2 \rightarrow O+N_2$	$k_7 = 1.8(-11)\exp(107/T)$

*Rates correspond to those recommended in DEMORE *et al.* (1985) [herein designated JPL-85-37].

†Spin conservation is not violated. $O_2(^1\Delta)$ is assumed to quench to O_2 rapidly.

‡$8.0(-12)$ means 8.0×10^{-12}.

transport of some other species to act as a source of catalytically active radicals. Also, the Chapman chemistry contains all of the essential feedbacks which exist because of the competition between O_2 and O_3 for ultraviolet photons. Thus, the so-called self-healing process is explicitly included.

Although Chapman chemistry leads to an overestimate of stratospheric ozone because of the neglect of H-, N- and Cl-catalyzed reactions leading to destruction of ozone, it is similar to the more complete chemistry. Like the more complete chemistry, the Chapman chemistry is not expected to be in PCE in the lower stratosphere, while in the upper stratosphere, where chemistry is fast, ozone production and loss should be in PCE.

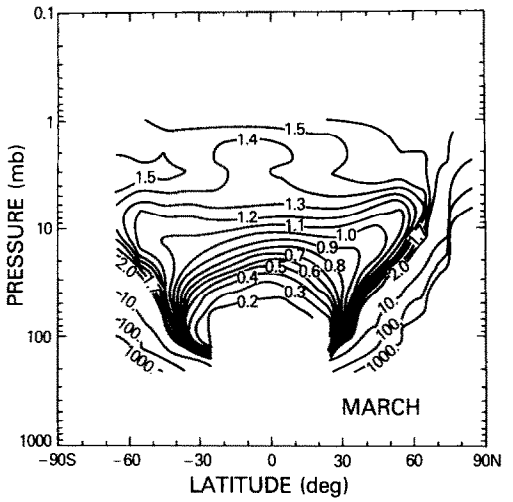

Fig. 1. Ozone loss/production (L/P) using LIMS and SAMS data in a two-dimensional monthly average photochemical equilibrium calculation for March (From fig. 12c, JACKMAN *et al.*, 1986).

OZONE PRODUCTION AND LOSS RATE CALCULATION AND COMPARISON

We first discuss the computation of production and loss rates of ozone using Nimbus 7 Limb Infrared Monitor of the Stratosphere (LIMS) (REMSBERG *et al.*, 1984; RUSSELL *et al.*, 1984a,b; GILLE *et al.*, 1984a,b) and Nimbus 7 Stratospheric and Mesospheric Sounder (SAMS) (JONES and PYLE, 1984) data. These calculations have been described in detail in our previous paper (JACKMAN *et al.*, 1986). Briefly, the LIMS data set included 7 months of nearly global data for temperature, O_3, NO_2, HNO_3 and H_2O. Methane was taken from the monthly average SAMS data set above 20 mb and from the 2D model computation of GUTHRIE and JACKMAN (1984) for altitudes below 20 mb. These two separate CH_4 data sets merge fairly smoothly with each other.

From these, quantities such as the diurnally averaged concentrations of $O(^3P)$, $O(^1D)$, N, NO, H, OH, HO_2, H_2O_2, NO_3, N_2O_5, HO_2NO_2 and others were derived under photochemical equilibrium assumptions. In these calculations the total amount of chlorine was taken from a 2D model calculation which used fluorocarbons 11 and 12 as surrogates for all chlorine sources and was normalized to give the best fit to the ClO measurements of MENZIES (1979) and ANDERSON and coworkers (ANDERSON *et al.*, 1980; WEINSTOCK *et al.*, 1983; BRUNE *et al.*, 1985). Figure 1 shows the loss/production (L/P) calculated in this manner by JACKMAN *et al.* (1986) for March 1979. Similar plots were given in that paper for other months.

Next, we use a simplified model calculation to simulate the observed atmosphere. We will investigate: (1) whether or not models will show the characteristic ozone production region in the lower stratosphere and (2) what factors this production region is dependent

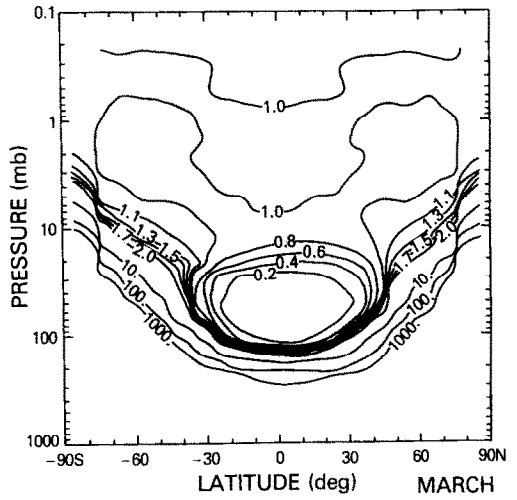

Fig. 2. Ozone loss/production (L/P) from a two-dimensional perpetual March with transport calculation using only Chapman chemistry.

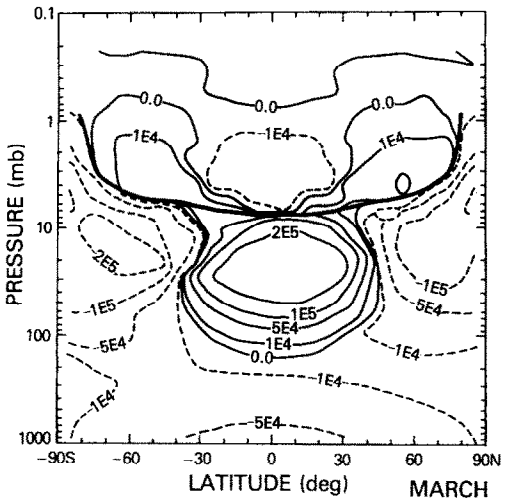

Fig. 3. Ozone production − loss ($P-L$) from a two-dimensional perpetual March with transport calculation using only Chapman chemistry. Negative regions are indicated by dashed contours. Heavy curve indicates peak of ozone distribution in a photochemical equilibrium condition.

upon. Figure 2 shows the calculated loss divided by production for the two-dimensional model of GUTHRIE *et al.* (1984) using only Chapman chemistry. These calculations are steady-state for perpetual March conditions. A notable feature of the calculation is the minimum in L/P, which reaches values less than 0.2 and is located in the same region as the minimum derived from the data. Figure 3 displays this information as $P-L$, thus illustrating the extension of the production region into the upper stratosphere at mid to high latitudes.

Table 2. Equatorial lifetime for destruction of ozone from the more complete chemistry model described in JACKMAN *et al.* (1986) and the Chapman chemistry model

Pressure (mbar)	Approximate height (km)	Full chemistry (days)	Chapman chemistry (days)
2	43	0.5	0.6
5	36	4	5
10	31	20	25
20	26	100	160
50	20	900	2500

This production region is located along the zone separating the photochemically dominated region and the dynamically dominated region and has been considered by many to be the principal region for net ozone production. Note that P does not exactly equal L in all of the photochemically dominated region. Both P and L have values close to 1×10^{7} cm^{-3} s^{-1} near 2 mbar at low latitudes. The quantity $P-L$, shown in Fig. 3, has a value between -1 and -5×10^{4} cm^{-3} s^{-1} near 2 mbar at low latitudes and thus is a very small residual of the competing production and loss terms. We are able to examine these small residual regions only in our idealized model calculation. In order to determine the relative importance of ozone production in the transition region (the region between the photochemically and dynamically dominated regions) and production in the equatorial lower stratosphere, a detailed understanding of the determining factors for net production or loss is required.

The nature of this transition region in both the more complete chemistry of JACKMAN *et al.* (1986) and the Chapman chemistry atmospheres is shown in Table 2. The equatorial ozone lifetimes for destruction are given at several altitudes. In particular, it is clear that in both cases PCE should be obeyed to a good approximation in the upper stratosphere for a zonally averaged model, where the ozone lifetime is shorter than a few days. In the lower stratosphere neither model should be in PCE, as photochemical time constants are much greater than a day. Both the more complete chemistry of JACKMAN *et al.* (1986) and the Chapman chemistry atmospheres have very similar ozone lifetimes at 10 mbar and above and qualitatively similar ozone lifetimes below 10 mbar.

The starting point for analysis of $P-L$ diagrams is photochemical equilibrium. If $P-L$ is zero then the ozone concentration will be equal to its photochemical equilibrium value. The production term is independent of the local ozone concentration, neglecting radiative feedback effects of O_3 on O_2. The loss term

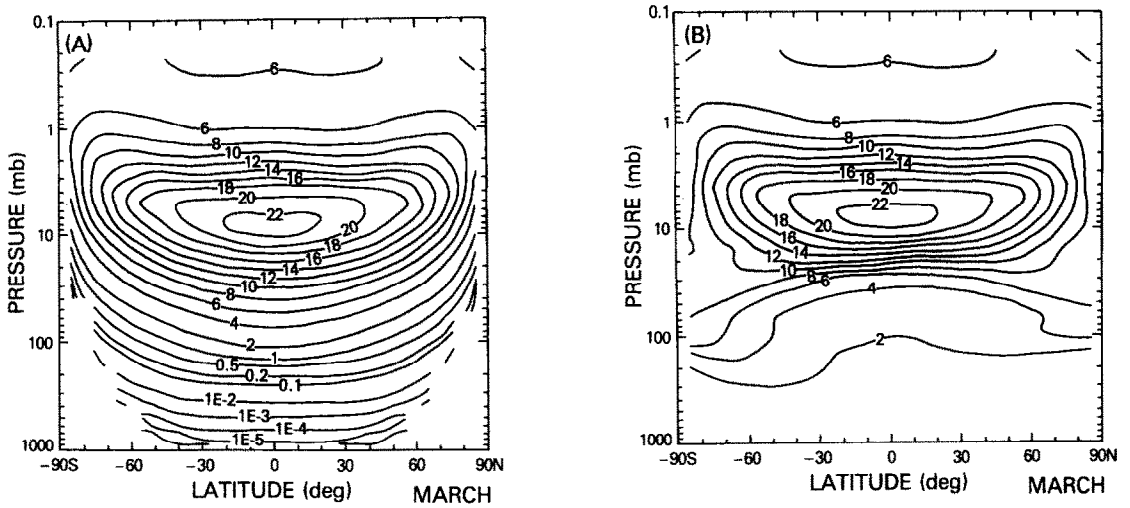

Fig. 4. (a) Ozone distribution from a two-dimensional perpetual March photochemical equilibrium condition calculation using only Chapman chemistry. (b) As (a), except perpetual March with transport.

in the real atmosphere varies from being proportional to ozone to being proportional to the square of ozone, depending on the chemistry (see discussion in the section Uncertainty Calculation, JACKMAN *et al.*, 1986). In Chapman chemistry the loss term is proportional to the square of ozone. Thus when ozone is in excess of its photochemical equilibrium value, the loss term will be enhanced over production and a negative $P-L$ will occur, which will tend to drive the ozone concentration downward toward photochemical equilibrium. The reverse is true when the ozone concentration is less than its local photochemical equilibrium value. The responsible factors for driving the ozone concentration away from photochemical equilibrium are the two other terms in the continuity equation, the time derivative and the flux divergence. The results shown in Fig. 3 were for a perpetual March simulation and thus contain no time-dependent terms. All departures from photochemical equilibrium are driven by the advection and diffusion terms in the model.

The ozone from the PCE perpetual March simulation is shown in Fig. 4a. The ozone from the perpetual March simulation which includes advection and diffusion is shown in Fig. 4b. Note that the peak of this Chapman chemistry ozone is about double the value of the ozone peak in the real atmosphere (see fig. 2, JACKMAN *et al.*, 1986, and references therein). The location of the peak, however, is about in the same place as in the real atmosphere (between 10 and 5 mbar).

The heavy line in Fig. 3 indicates the location of the peak value of the photochemical equilibrium solution of the O_3 mixing ratio for the PCE perpetual March case. Note the nearly exact pairing of net production and net loss regions above and below the line. This distribution reflects the primarily advective dynamics of the GUTHRIE *et al.* (1984) model. In equatorial regions the circulation is upward. Above the mixing ratio peak the flow is bringing air into the region which has more ozone than the local photochemical equilibrium (compare Figs. 4a, b) and hence the loss term increases to attempt to reduce ozone toward its PCE solution. Below the peak the reverse is true and a net production results.

At higher latitudes the circulation turns over and the downward motions produce the same effect with the opposite sign. Above the peak the pattern is strongly dominated by the vertical motions as indicated, because the horizontal gradient of the PCE solution is small. Below the peak significant horizontal gradients appear and contribute to the determination of the departure from PCE. Thus advective transport results in a change in the sign of $P-L$ at the peak of the PCE solution.

Diffusion will transport ozone down the gradient of the mixing ratio and thus results in a net production region centered on the peak of the PCE solution. This is shown in Fig. 5a, which gives L/P for the same model but with advection, horizontal diffusion (K_{yy}), K_{yz} and K_{zy} turned to zero. Thus transport is accomplished only by vertical diffusion (K_{zz}) and K_{zz} is 2×10^3 cm^2 s^{-1} above 100 mbar, a very small number. K_{zz} increases with higher pressures below 100 mbar and is 1×10^4 cm^2 s^{-1} at 300 mbar and below. Figure 5b shows the same result when only

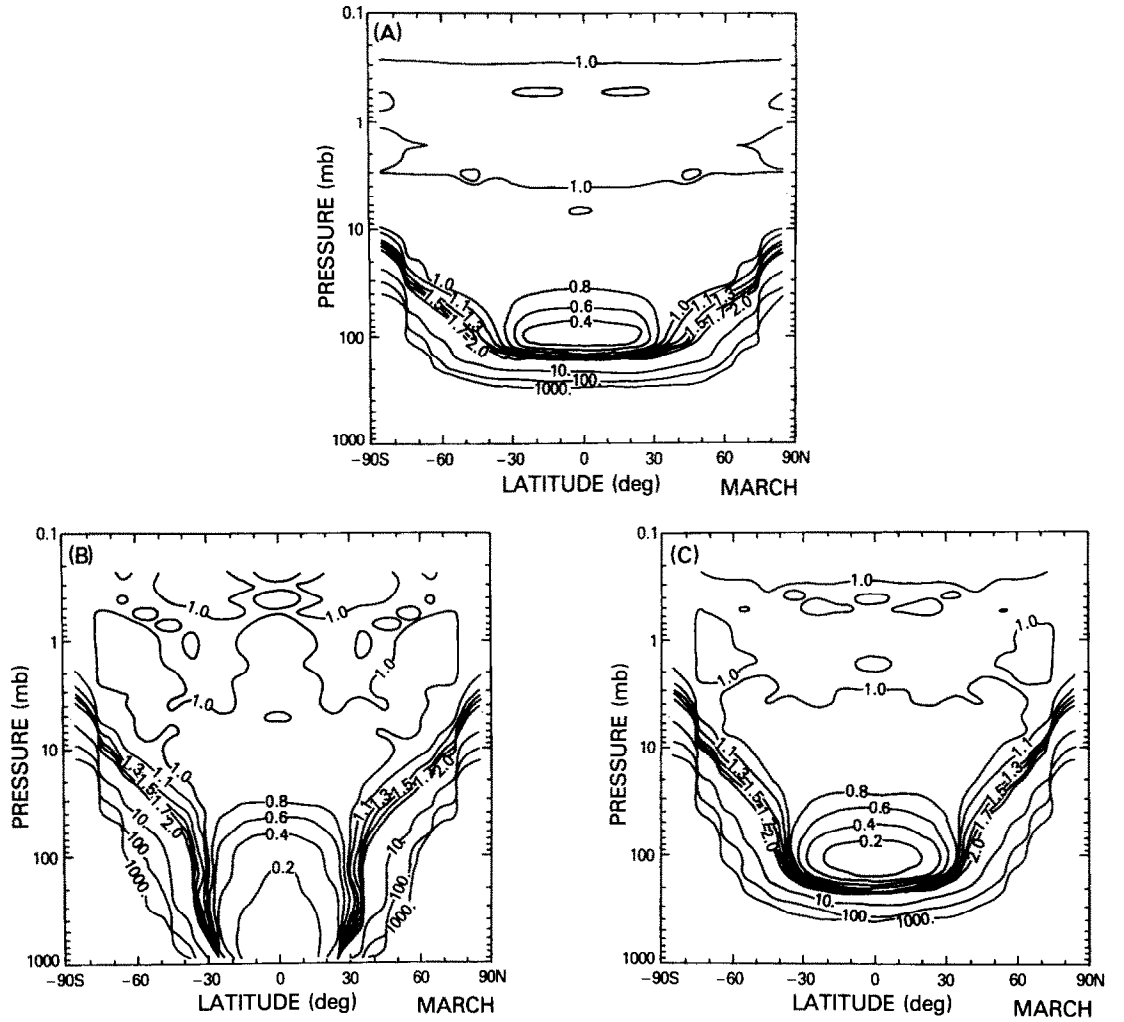

Fig. 5. (a) Ozone loss/production (L/P) from a two-dimensional perpetual March with only vertical diffusion (no advection) using only Chapman chemistry. (b) As (a), except perpetual March with only horizontal diffusion. (c) As (a), except perpetual March with both vertical and horizontal diffusion.

horizontal diffusion (K_{yy}) is allowed at 2×10^{9} cm^2 s^{-1} above 100 mbar. K_{yy} increases with higher pressures below 100 mbar and is 1×10^{10} cm^2 s^{-1} at 300 mbar and below. Figure 5c shows the same result when both K_{yy} and K_{zz} are allowed. The gross features of the L/P inferred for the real atmosphere are preserved, namely the region in the low latitude lower stratosphere where L/P is significantly less than one and the region at high latitudes in the lower stratosphere where L/P is significantly more than one. Note that in the upper stratosphere (less than 10 mbar) at all tropical and mid-latitudes L/P is very close to one, indicating that the PCE condition holds quite well there.

Figure 6 shows the calculated $P-L$ for the model run with perpetual June or solstice conditions, including transport due to all processes. An asymmetry is observed because of the sun position at this time of year. Again, however, the break between net production and net loss regions follows closely the peak of the calculated PCE solution as indicated by the heavy solid line.

To evaluate the relative importance of the time derivative term as compared to the flux divergence term in driving the ozone concentration away from PCE, a seasonal run was made with the same chemistry and transport. The resulting $P-L$ for day 77 (March) and day 190 (June) are shown in Fig. 7a, b. The way in which the time derivative term affects $P-L$ is by having the sun progress in its march through the

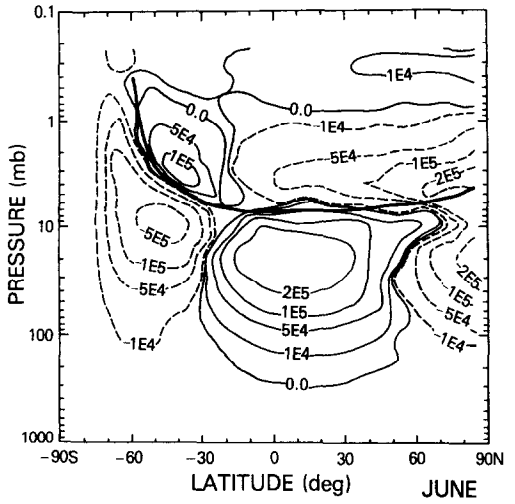

Fig. 6. Ozone production−loss ($P-L$) for a two-dimensional perpetual June with transport calculation using only Chapman chemistry. Negative regions are indicated by dashed contours. Heavy curve indicates peak of ozone distribution in a photochemical equilibrium condition.

seasons fast enough that the changes in the PCE solution are rapid and the ozone concentration cannot adjust. This has clearly happened in March, where in the northern upper stratosphere the model is trying to remove ozone to lower the concentration from its high winter-time values. Thus a loss region occurs where the perpetual March run showed net production. The seasonal run in June, however, shows almost exactly the same pattern as the perpetual June run, as was shown in Fig. 6. The magnitude of the net production or loss is somewhat different, but the similarity in shape suggests that for diagnosis of the behavior of the chemistry–transport interaction in a 2D model a seasonal run may not be necessary.

CONCLUSIONS

We find that similarities exist between ozone L/P plots calculated using satellite data and a photochemical equilibrium model and ozone L/P plots calculated using Chapman chemistry in a two-dimensional model. These similarities indicate that Chapman chemistry can be used to study gross features in the deviation of stratospheric ozone concentrations from their photochemical equilibrium values. Transport can drive ozone either above or below its PCE condition resulting in net photochemical loss or production, respectively. Computation of net production of ozone and other species should prove to be a sensitive diagnostic of model behavior.

We also find that a two-dimensional model with only vertical and horizontal diffusion and no advection can also produce gross features in ozone L/P similar to those inferred for the atmosphere from a combination of data and a PCE model. This means that significant care must be taken in interpreting these diagnostics, because two-dimensional models with vastly different transport schemes (say, one dominated by advection and the other dominated by diffusion) can lead to ozone climatologies which are similar in gross features to each other and to that

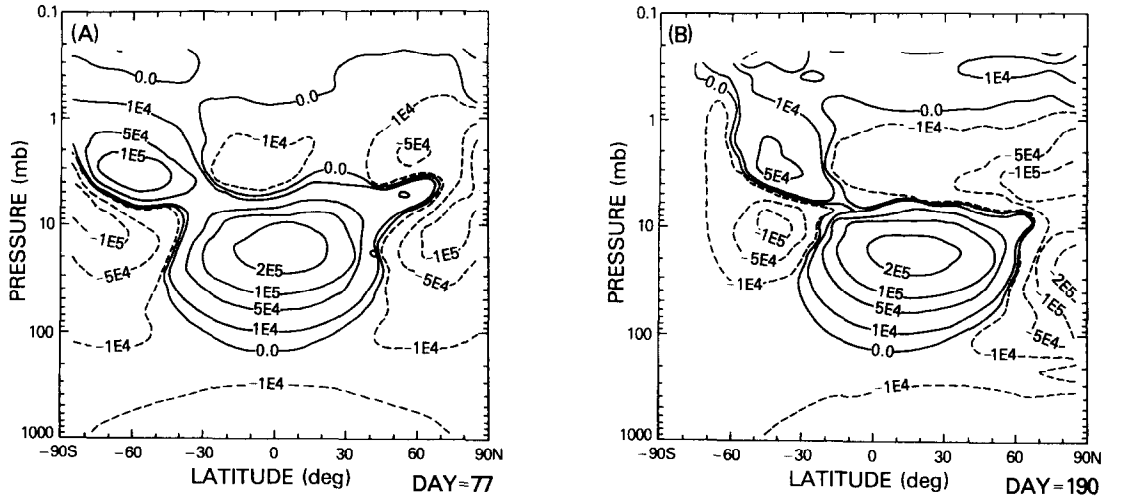

Fig. 7. Ozone production−loss ($P-L$) for a two-dimensional time dependent run. Negative regions are indicated by dashed contours. (a) Day 77 (March) and (b) day 190 (June) of the run.

inferred from data. A correct transport scheme cannot be determined from only a comparison between the model output and the inferred ozone L/P. Other quantities, such as the divergence of the flux of ozone and the time rate of change of ozone or of other minor species, must be investigated as well.

REFERENCES

Anderson J. G., Grassl H. J., Shetter R. E. and Margitan J. J.	1980	*J. geophys. Res.* **85,** 2869.
Brune W. H., Weinstock E. M., Schwab M. J., Stimpfle R. M. and Anderson J. G.	1985	*Geophys. Res. Lett.* **12,** 441.
Crutzen P. J. and Schmailzl U.	1983	*Planet. Space Sci.* **31,** 1009.
DeMore W. B., Margitan J. J., Molina M. J., Watson R. T., Golden D. M., Hampson R. F., Kurylo M. J., Howard C. J. and Ravishankara A. R.	1985	Chemical kinetics and photochemical data for use in stratospheric modeling, JPL Publication 85-37, Jet Propulsion Laboratory, Pasadena, CA.
Frederick J. E., Serafino G. N. and Douglass A. R.	1984	*J. geophys. Res.* **89,** 9547.
Gille J. C., Russell J. M., Bailey P. L., Remsberg E. E., Gordley L. L., Evans W. F. J., Fischer H., Gandrud B. W., Girard A., Harries J. E. and Beck S. A.	1984a	*J. geophys. Res.* **89,** 5179.
Gille J. C., Russell J. M., Bailey P. L., Gordley L. L., Remsberg E. E., Lienesch J. H., Planet W. G., House F. B., Lyjak L. V. and Beck S. A.	1984b	*J. geophys. Res.* **89,** 5147.
Guthrie P. D. and Jackman C. H.	1984	*EOS Trans. Am. geophys. Un.* **65,** 834.
Guthrie P. D., Jackman C. H., Herman J. R. and McQuillan C. J.	1984	*J. geophys. Res.* **89,** 9589.
Jackman C. H., Stolarski R. S. and Kaye J. A.	1986	*J. geophys. Res.* **91,** 1103.
Jones R. L. and Pyle J. A.	1984	*J. geophys. Res.* **89,** 5263.
Menzies R. T.	1979	*Geophys. Res. Lett.* **6,** 151.
Remsberg E. E., Russell J. M., Gille J. C., Gordley L. L., Bailey P. L., Planet W. G. and Harries J. E.	1984	*J. geophys. Res.* **89,** 5161.
Russell J. M., Gille J. C., Remsberg E. E., Gordley L. L., Bailey P. L., Fischer H., Girard A., Drayson S. R., Evans W. F. J. and Harries J. E.	1984a	*J. geophys. Res.* **89,** 5115.
Russell J. M., Gille J. C., Rembserg E. E., Gordley L. L., Bailey P. L., Drayson S. R., Fischer H., Girard A., Harries J. E. and Evans W. F. J.	1984b	*J. geophys. Res.* **89,** 5099.
Weinstock E. M., Phillips M. J. and Anderson J. G.	1981	*J. geophys. Res.* **86,** 7273.